Atmos. Chem. Phys., 25, 9263–9274, 2025
https://doi.org/10.5194/acp-25-9263-2025

Atmospheric Chemistry and Physics
Open Access
EGU

Measurement report: Polycyclic aromatic hydrocarbons (PAHs) and their alkylated (RPAHs), nitrated (NPAHs), and oxygenated (OPAHs) derivatives in the global marine atmosphere – occurrence, spatial variations, and source apportionment

Rui Li[1,2,★], **Xing Liu**[3,★], **Yubing Shen**[1], **Yumeng Shao**[1], **Yining Gao**[1], **Ziwei Yao**[3], **Xi Liu**[4], and **Guitao Shi**[1]

[1]Key Laboratory of Geographic Information Science of the Ministry of Education, School of Geographic Sciences, East China Normal University, Shanghai, 200241, China
[2]Institute of Eco-Chongming (IEC), 20 Cuiniao Road, Chenjia Town, Chongming District, Shanghai, 202162, China
[3]State Environmental Protection Key Laboratory of Coastal Ecosystem, National Marine Environmental Monitoring Center, Dalian, 116023, China
[4]Agilent Technologies (China) Ltd., Inc., Beijing, 100102, China
★These authors contributed equally to this work.

Correspondence: Rui Li (rli@geo.ecnu.edu.cn) and Guitao Shi (gtshi@geo.ecnu.edu.cn)

Received: 29 November 2024 – Discussion started: 3 February 2025
Revised: 6 June 2025 – Accepted: 6 June 2025 – Published: 26 August 2025

Abstract. Ambient polycyclic aromatic hydrocarbons (PAHs) and their derivatives have severe adverse impacts on organism health and ecosystem safety. However, their global distributions, sources, and fate in marine aerosol remain poorly understood. To fill the knowledge gap, high-volume air samples were collected along a transect from China to Antarctica and analyzed for particulate PAHs and derivatives. The highest PAH concentrations in marine aerosols were observed in the Western Pacific (WP: $447 \pm 228\,pg\,m^{-3}$), followed by the East China Sea (ECS: $195\,pg\,m^{-3}$), the Antarctic Ocean (AO: $111 \pm 91\,pg\,m^{-3}$), the East Australian Sea (EAS: $104 \pm 88\,pg\,m^{-3}$), and (the lowest) the Bismarck Sea (BS: $17 \pm 12\,pg\,m^{-3}$). Unexpectedly, PAH concentrations in the AO were even higher than those in the EAS and BS. This could be attributed to the relatively low anthropogenic PAH emissions from Australia and Papua New Guinea, whereas AO is often affected by emissions from engine combustion and biomass burning. In contrast to the distribution of PAHs, OPAH levels in the EAS were much higher than those in the AO. It was assumed that OPAHs mainly originated from the secondary formation of parent PAHs through reactions with O_3 and OH radicals, both of which are more prevalent in the EAS. Several source apportionment models suggested that PAHs and their derivatives in marine aerosol are dominated by three sources: coal burning and engine combustion emissions (56 %), wood and biomass burning (30 %), and secondary formation (14 %). Specifically, marine aerosols in the ECS and WP were significantly affected by coal burning and engine combustion, while those in the BS and EAS were mainly influenced by wildfire and coal combustion. AO was primarily dominated by biomass burning and local shipping emissions.

Published by Copernicus Publications on behalf of the European Geosciences Union.

1 Introduction

Polycyclic aromatic hydrocarbons (PAHs), a class of semi-volatile organic compounds (SVOCs), are often considered carcinogenic and mutagenic pollutants (Li et al., 2023; Wei et al., 2021). These pollutants are generally released from the combustion of fossil fuels, biofuels, oil spills, and other biogenic sources (Li et al., 2021a; Zhang et al., 2023). Due to long-range atmospheric transport (LRAT), PAHs emitted from industrial and residential sources can often be transported to remote regions such as the open ocean and polar areas (Li et al., 2021a; Zhang et al., 2023). These PAHs species can exert toxic effects on marine organisms through dry and wet deposition (Li et al., 2021b). Additionally, high levels of oxidants (OH radicals, NO_3 radicals, and O_3) enriched in the atmosphere can promote the transformation of parent PAHs into their alkylated, nitrated, and oxygenated derivatives (RPAHs, NPAHs, and OPAHs, respectively) (Zimmermann et al., 2013). Compared to parent PAHs, nearly all of these derivatives exhibit higher toxic potency to aquatic animals due to their direct-acting mutagenicity (Bandowe and Meusel, 2017; Kovacic and Somanathan, 2014). Therefore, it is crucial to investigate the spatial characteristics of PAHs and their derivatives and to identify the key factors and potential sources of atmospheric PAHs. This knowledge is essential for reducing potential damage to ocean ecosystems and improving marine environmental management.

A growing body of literature has explored the spatial variations of ambient PAHs in the marine atmosphere. For instance, Kang et al. (2017) found that atmospheric PAH concentrations in the East China Sea ranged from 0.16–17.6 $ng\,m^{-3}$ (average: 3.87 $ng\,m^{-3}$), with these compounds being dominated by 4-ring PAHs. Subsequently, Neroda et al. (2020) investigated PAHs in the aerosols of the North-West Pacific Ocean, estimating total PAH levels ranging from 17.1 $pg\,m^{-3}$ (northern part of the Sea of Japan) to 142 $pg\,m^{-3}$ (La Perouse Strait). More recently, Wietzoreck et al. (2022) reported that the mean concentrations of total PAHs, RPAHs, OPAHs, and NPAHs in the gas and particulate phases in the Mediterranean were 2.99 ± 3.35, 0.83 ± 0.87, 0.24 ± 0.25, and 4.34 ± 7.37 $pg\,m^{-3}$, respectively. Most current studies about PAHs in marine aerosols focus on regional scales, particularly in oceans with intense anthropogenic activities, while few studies reveal the spatial distributions of PAHs and their derivatives in remote oceans (e.g., the polar oceans) or on a global scale. The Southern Ocean is often considered a remote and pristine sea, and its local ecosystem is more sensitive to PAHs and their derivatives. However, to date, only a few studies have investigated the spatial variations of ambient PAHs in the marine aerosol within this region. Cabrerizo et al. (2014) first demonstrated that the volatilization from soil and snow might be the major sources of ambient PAHs in the Southern Ocean and Antarctica. Very recently, Van Overmeiren et al. (2024) analyzed the components of PAHs and OPAHs at a coastal site in Antarctica and found that phenanthrene, pyrene, and fluoranthene derived from volcanic emissions accounted for the major fractions of PAHs. To the best of our knowledge, only Zhang et al. (2022) investigated the global variations of PAH components in marine aerosols and found a clear latitudinal gradient from the Western Pacific to the Southern Ocean. They also identified coal combustion as the major contributor to ambient PAHs (52 %). Zetterdahl et al. (2016) also revealed that shipping emissions might play an important role for PAHs in the marine atmosphere. They verified that the new regulation (since late 2014) about the use of low-sulfur residual marine fuel oil instead of heavy oil significantly altered the chemical compositions of PAHs (increasing the low-ring components while decreasing the high-ring components). Unfortunately, nearly all current studies focus solely on PAHs and OPAHs in regional oceans, whereas no study has comprehensively investigated the spatial variations of particulate PAHs and all their derivatives on a global scale. Moreover, the source contributions of PAH derivatives in different oceans remain unknown. It is important to fill the knowledge gaps regarding the compositions, sources, and fate of PAH derivatives in the marine atmosphere on a global scale.

In our study, an expedition research cruise aboard a Chinese research vessel from October 2019–April 2020, traveling from China to Antarctica, provided a unique opportunity to reveal the distributions, compositions, and fate of parent PAHs and their derivatives (RPAHs, NPAHs, and OPAHs). Taking advantage of this unique opportunity, our study aims to (1) investigate the latitudinal gradient of PAHs and their derivatives, (2) study the major factors contributing to the spatial variations, and (3) identify the sources using a positive matrix factorization (PMF) model.

2 Material and methods

2.1 The shipping cruise and sample collection

The research expedition of the Chinese research vessel took place from 22 October 2019–21 April 2020. The expedition sailed from Shanghai in China, crossing the Pacific, Indian Ocean, and Southern Ocean, and finally arrived at Antarctica. Then, the return route was also from Antarctica to Shanghai, in China. Detailed information on the shipping route is depicted in Figs. 1 and S1 in the Supplement.

Atmospheric samples were collected using a high-volume air sampler (HVAS, TISCH Environmental, USA), positioned on the upper deck of the RV *Xuelong*, approximately 30 m above sea level. Aerosol particles were captured on Whatman quartz fiber filters (QM-A, 20.3 cm × 25.4 cm, pore size 2.5 µm), which were pre-baked at around 500 °C for over 4 h to eliminate water and organic residues. The HVAS operated at an airflow rate of approximately 1.2 $m^3\,min^{-1}$, with each sampling event lasting 2–3 d, resulting in total air volumes typically ranging from 3000–4000 m^3. During this time, atmospheric particles were collected along the cruise

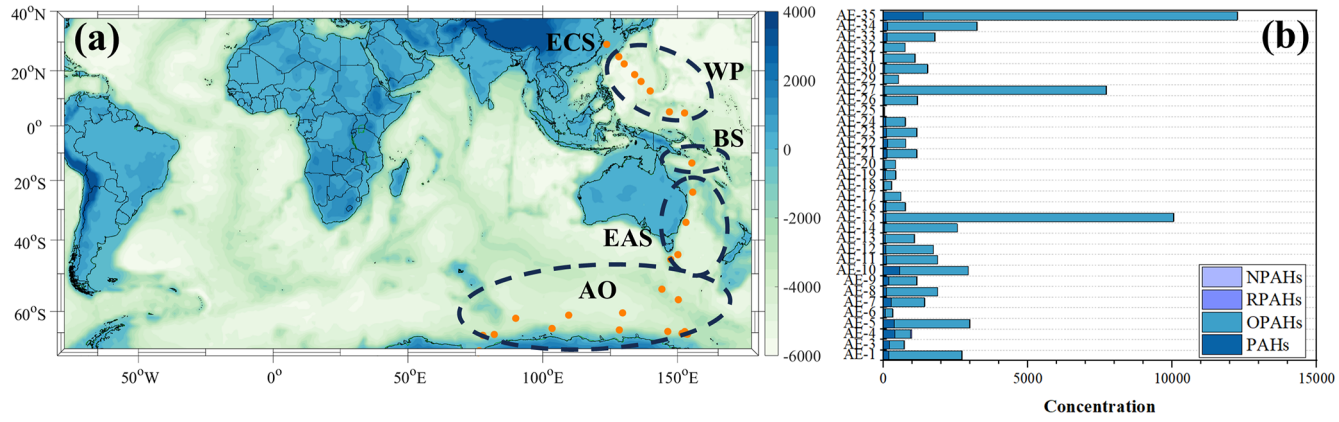

Figure 1. The sampling sites during the cruise from Shanghai to Antarctica (orange dots) **(a)**. The total concentrations (unit: pg m^{-3}) of PAHs, OPAHs, RPAHs, and NPAHs for all of the samples (from AE-1 to AE-35) **(b)**. The indicators from AE-1 to AE-35 represent the collected aerosol samples in the global marine environment. ECS, WP, BS, EAS, and AO represent East China Sea, Western Pacific, Bismarck Sea, Eastern Australia Sea, and Antarctic Ocean, respectively. Publisher's remark: please note that the above figure contains disputed territories.

path, spanning approximately 2–4° of latitude, yielding a single aggregate sample per filter. To minimize potential contamination from the research vessel, a wind direction sensor directed the HVAS, ensuring that only air masses from a sector of approximately 120° on either side of the vessel's central trajectory were sampled. After collection, individual filters were carefully separated, folded, wrapped in aluminum foil, placed in ziplock bags, and stored in the dark at −20 °C until particle characterization analyses began. A total of 35 samples were collected during the cruise, along with two field blank samples prepared from filters mounted in the HVAS with an air pump flow rate set to 0. The sampling protocols for the blanks mirrored those described above regarding duration, filter mounting, collection, transport, observation, and measurements.

2.2 Chemical analysis

Automated Soxhlet extraction with DCM (JT Baker, Avantor group, Poland, pesticide residue grade) in a B-811 extraction unit (Büchi, Flawil, Switzerland) for PAH, NPAH, and OPAH analyses was employed. The extract was cleaned up using a silica column (with 1 cm i.d. as open tube using 5 g of silica (Merck, Darmstadt, Germany), 0.063–0.200 mm, activated at 150 °C for 12 h, 10 % deactivated with water) and 1 g Na_2SO_4 (Merck, Darmstadt, Germany). For the analysis of RPAHs, $PM_{2.5}$ samples were extracted based on the procedure described in Iakovides et al. (2021). A gas chromatograph (Agilent 7890B GC) coupled with a mass spectrometer (Agilent 5977B MS) was employed to determine the concentrations of PAH, NPAH, and OPAH species. The detailed analysis method and quality control of these PAHs and their derivatives are introduced in the Supplement (Sect. S1 and Table S1 in the Supplement). The reference standards of PAHs (Pyr-d10 and BaP-d12; Wako Pure Chemicals, Osaka, Japan), OPAHs (purchased from First Standard, Sigma, America), RPAHs (AccuStandard; New Haven, CT, USA), and NPAHs (2-fluoro-7-nitrofluorene; Aldrich Chemical Company, Osaka, Japan) were used for calibrating the quantification.

2.3 Source apportionment

As a typical receptor-based model used for source apportionment, the PMF 5.0 version has been widely applied to determine the potential origins of PAH and their derivatives, as well as to determine the contribution ratios of multiple sources to these components (Sharma et al., 2016). The aim of the PMF model is to solve the issues of chemical mass balance between the observed concentration of each PAH species and their source contributions via decomposing the input matrix into factor contributions and factor profiles. The detailed equation is shown in Eq. (1). Additionally, the contribution of each source for an individual component should be ensured to be non-negative. Briefly, the basic principle of PMF is to determine the least object function Q when g_{ik} is a non-negative matrix based on Eq. (2) (Jaeckels et al., 2007; Taghvaee et al., 2018).

$$x_{ij} = \sum_{k=1}^{p} g_{il} f_{lj} + e_{ij}, \tag{1}$$

$$Q = \sum_{i=1}^{n} \sum_{j=1}^{m} \left[\frac{x_{ij} - \sum_{k=1}^{p} g_{il} f_{lj}}{u_{ij}} \right]^2, \tag{2}$$

where x_{ij} and e_{ij} represent the PAH concentrations and uncertainty of the jth component, respectively. g_{il} denotes the contribution ratio of the lth source to the ith sample, f_{lj} is

the ratio of the jth component in the lth source, and e_{ij} denotes the residual of the jth element in the ith sample. The 2- to 6-factor solutions were examined, and a three-factor solution was decided on with the ratio of Q (robust) and Q (true) reaching 0.93. The coefficients of determination (R^2) between the predicted and observed concentrations of PAHs and their derivatives are shown in Table S2. The uncertainties linked with factor profiles were assessed based on three error calculation methods, including the bootstrap (BS) method, displacement (DISP) analysis, and the combination method of DISP and BS (BS-DISP). For the BS method, 1000 runs were conducted, and the result is considered to be robust as all of the factors showed a mapping of above 90 %. DISP analysis also demonstrated that this solution was stable as the observed drop in the Q value was < 0.1 %, and no factor swap occurred. For the BS-DISP analysis, the solution was verified to be useful as the observed drop in the Q value was < 0.5 %. Moreover, the results from both BS and BS-DISP did not show any asymmetry or rotational ambiguity for all of the factors (Ambade et al., 2023; Gao et al., 2015; Yan et al., 2017).

2.4 GEOS-Chem model

The GEOS-Chem (v13.4.0) model was employed to estimate O_3 and OH radical concentrations during 1 January–31 December in 2019. This model comprises a complex chemistry mechanism of tropospheric NO_x–VOC–O_3–aerosol (Park et al., 2004). This model was driven by MERRA2 meteorological parameters (Hamal et al., 2020; Koster et al., 2020; Qiu et al., 2020). A global simulation was conducted at a spatial resolution of $2° \times 2.5°$ (Qiu et al., 2020; Weagle et al., 2018; Zhang et al., 2021a). The historical multi-sector anthropogenic emission dataset was downloaded from the Community Emissions Data System (Hoesly et al., 2018). Natural emissions including wildfire, soil, and lightning emissions were also incorporated into the GEOS-Chem model. Wildfire emissions derived from the Global Fire Emissions Database (GFED) were used for simulations (Chen et al., 2023). The lightning NO_x emissions were collected from http://geoschemdata.wustl.edu/ExtData/HEMCO/OFFLINE_LIGHTNING/v2020-03/MERRA2/, last access: 25 May 2025 (Murray et al., 2012).

3 Results and discussions

3.1 The chemical compositions of PAHs and their derivatives in the atmosphere

The concentrations of 18 PAHs, 11 OPAHs, 9 RPAHs, and 7 NPAHs in 33 samples were determined. The average concentrations of Σ PAHs, Σ OPAHs, Σ RPAHs, and Σ NPAHs were 157 ± 98, 1920 ± 1250, 12.1 ± 9.5, and 3.0 ± 1.6 pg m^{-3}, respectively. The total concentrations of PAHs and their derivatives in the marine aerosols (Pacific and Antarctic Ocean (AO)) were significantly lower than those in urban regions such as Harbin (86.9 ng m^{-3}) (Ma et al., 2020), Augsburg (1.3 ng m^{-3}) (Pietrogrande et al., 2011), or southeastern Florida (3.0 ng m^{-3}) (Sevimoglu and Rogge, 2016). However, the PAH concentration in our study was comparable to those in some remote regions. For instance, Cabrerizo et al. (2014) found that the total concentration of 18 particulate PAHs over AO ranged from 0.03–4.2 ng m^{-3}. Later on, Zhang et al. (2022) reported that the 15 PAHs in $PM_{2.5}$ across the Pacific and AO ranged from 0.11–1.2 ng m^{-3}. Very recently, Van Overmeiren et al. (2024) revealed that the total concentrations of 15 PAHs in $PM_{2.5}$ in Antarctica was only 1.5 pg m^{-3}, which was even lower than the result in our study. The large gaps for PAH concentrations between remote ocean (polar region) and urban regions might be associated with the intensity of anthropogenic emissions (Shen et al., 2013; Zhang and Tao, 2009). Although the total concentration could provide the overall picture of PAHs in the global marine boundary layer, the specific compounds in PAHs also varied greatly.

Among all of the PAHs, BbF (Benz[b]fluoranthene) showed the highest level (26.8 ± 10.4 pg m^{-3}), followed by Ace (Acenaphthylene) (18.4 ± 9.8 pg m^{-3}), Fluoran (16.3 ± 8.4 pg m^{-3}), and (the lowest one) Acy (0.12 ± 0.05 pg m^{-3}) (Fig. 2). Overall, the PAHs in the global marine aerosols were dominated by 3- to 5-ring components (~ 83 %), which was in agreement with the result in the Pacific and Indian Ocean observed by Zhang et al. (2022). It was reported that Fluoran, Acy, and Ace were often sourced from biomass or coke burning (Zhang et al., 2021c), while BbF was generally enriched in the production of wood and coal combustion (Li et al., 2022), indicating that the marine aerosol could be influenced by solid fuel burning.

Among all of the OPAHs, 1-Naphthaldehyd showed the highest concentration (852 ± 406 pg m^{-3}), followed by 1,4-Chysenequione (787 ± 386 pg m^{-3}), Ancenaphthenaquinone (133 ± 75 pg m^{-3}), Anthraquinone (58 ± 31 pg m^{-3}), and (the lowest one) 5,12-Naphthacenequione (1.49 ± 0.64 pg m^{-3}). In general, the absolute concentrations of OPAHs were comparable or slightly lower than those of PAHs, especially in some high-latitude sites. Nevertheless, the OPAH concentrations in our study were markedly higher than PAH levels ($p < 0.01$). It is well known that OPAHs are often released from incomplete combustion or generated from photochemical reactions of O_3, OH, and NO_3 radicals with PAHs (Zhang et al., 2022). The higher concentrations of O_3 and OH radicals over tropical oceans might largely promote the PAH oxidation (Zhang et al., 2022). For RPAHs, 1,3-Dimethylnaphthalene (4.47 ± 2.64 pg m^{-3}) and 2-Methylnaphthalene (4.38 ± 2.42 pg m^{-3}) accounted for the major fractions (73 %) of RPAHs, while the concentrations of other species were relatively low. Wietzoreck et al. (2022) confirmed that the chemical compositions of RPAHs in Middle East seas displayed similar patterns when compared with our study. The NPAHs in the marine aerosol were

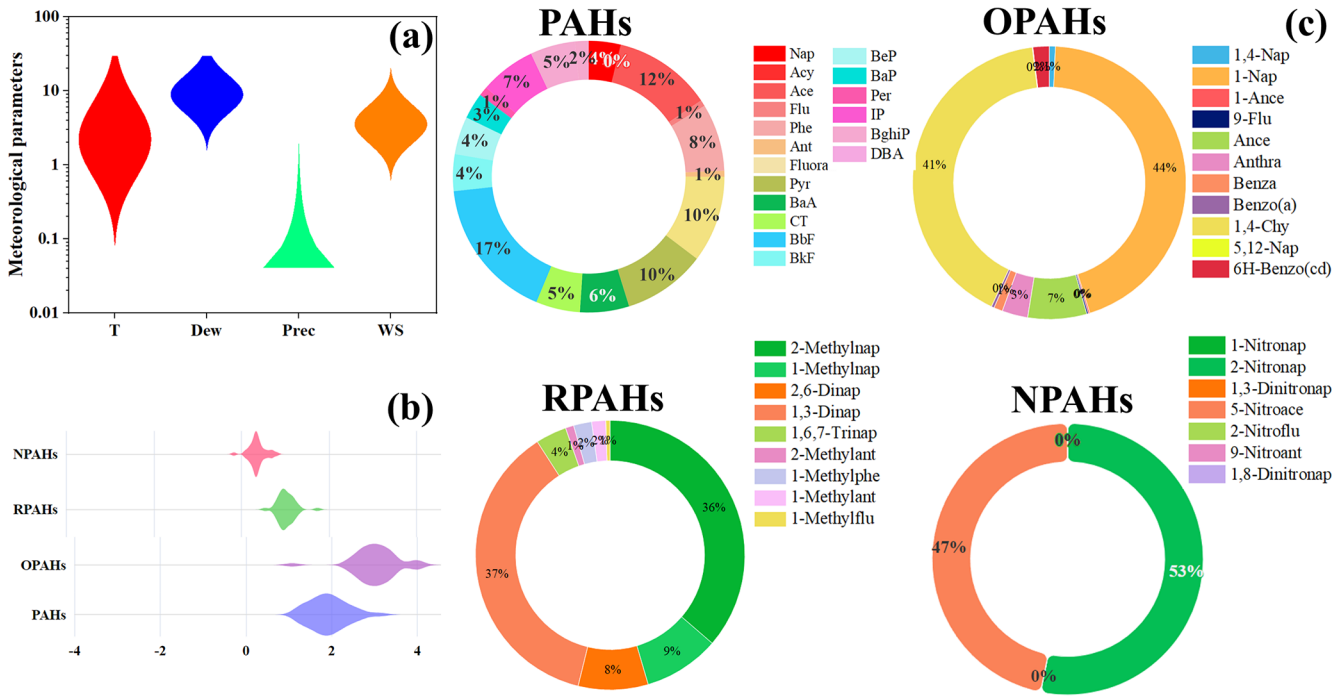

Figure 2. The average meteorological parameters during the cruise **(a)**. T, Dew, Prec, and WS denote 2 m air temperature (unit: °C), dewpoint temperature (unit: °C), precipitation (mm), and wind speed ($m\,s^{-1}$), respectively. The average concentrations (log_{10} (concentration), unit: $pg\,m^{-3}$) of PAHs, OPAHs, RPAHs, and NPAHs for all of the samples **(b)**. The contribution ratios of species in PAHs, OPAHs, RPAHs, and NPAHs (unit: %) **(c)**. For OPAHs, 1,4-Nap, 1-Nap, 1-Ance, 9-Flu, Ance, Anthra, Benza, Benzo(a), 1,4-Chy, 5,12-Nap, and 6H-Benzo(cd) represent 1,4-Naphthoquinone, 1-Naphthaldehyde, 1-Ancenaphthenaquinone, 9-Fluorenone, Ancenaphthenaquinone, Anthraquinone, Benzanthrone, Benzo(a) anthracene-7,12-dione, 1,4-Chysenequione, 5,12-Naphthacenequione, and 6H-Benzo(cd)pyrene-6-one, respectively. For RPAHs, 2-Methylnap, 1-Methylnap, 2,6-Dinap, 1,3-Dinap, 1,6,7-Trinap, 2-Methylant, 1-Methylphe, 1-Methylant, and 1-Methylflu denote 2-Methylnaphthalene, 1-Methylnaphthalene, 2,6-Dimethylnaphthalene, 1,3-Dimethylnaphthalene, 1,6,7-Trimethylnaphthalene, 2-Methylanthracene, 1-Methylphenanthrene, 1-Methylanthracene, 1-Methylfluoranthene, respectively. For NPAHs, 1-Nitronap, 2-Nitronap, 1,3-Dinitronap, 5-Nitroace, 2-Nitroflu, 9-Nitroant, and 1,8-Dinitronap reflect 1-Nitronaphthalene, 2-Nitronaphthalene, 1,3-Dinitronaphthalene, 5-Nitroacenaphthene, 2-Nitrofluorene, 9-Nitroanthracene, and 1,8-Dinitronaphthalene, respectively.

also dominated by 2-Nitronaphthalene ($2.2 \pm 1.1\,pg\,m^{-3}$) and 5-Nitroacenaphthene ($2.0 \pm 0.7\,pg\,m^{-3}$), while the contributions of other species were negligible.

3.2 The spatial variations of particulate PAH derivatives and key meteorological factors

To reveal the spatial variations of atmospheric PAHs and their derivatives, all of the sampling sites were divided into five groups (regions): East China Sea (ECS), Western Pacific (WP), Bismarck Sea (BS), Eastern Australia Sea (EAS), and Antarctica Ocean (AO). The PAH concentrations followed the order of WP ($447 \pm 228\,pg\,m^{-3}$) > ECS ($195\,pg\,m^{-3}$) > AO ($111 \pm 91\,pg\,m^{-3}$) > EAS ($104 \pm 88\,pg\,m^{-3}$) > BS ($17 \pm 12\,pg\,m^{-3}$) (Fig. 3). Based on a Mann–Whitney test, the PAH concentrations in the WP were significantly higher than those in other oceans ($p < 0.05$). High levels of PAHs in the WP are closely linked with the high coverage of continent-affected regions such as Southeast Asian and East Asian countries. AO showed the lower PAH concentrations, because the sea was far away from continental sources. In general, PAH levels in the remote marine atmosphere appear to be affected by long-range transport and air–seawater exchange, whereas local anthropogenic emissions might be responsible for the ambient PAHs near the continent. For the AO, the Antarctic continent lacks anthropogenic activity; thus, this leads to the lower PAH levels in the atmosphere of AO. It should be noted that both EAS and BS were close to Australia, while the PAH concentrations in these oceans were even lower than those in the AO. It was assumed that Australia possesses very low anthropogenic PAH emissions ($< 10\,\mu g\,km^{-2}$) compared with many other continents (Shen et al., 2013). Although the total PAHs showed remarkably higher concentrations in the ECS and WP, all of the congeners did not show the same spatial variations with the total PAH levels. For instance, Fluoran, Pyr, BeP, and BaP levels in the AO were even higher than those in the ECS, and the BbF levels in the EAS were much higher than those in the ECS. BbF generally originated from wood burning (Zhang et al., 2022a), and wildfire often occurred in the

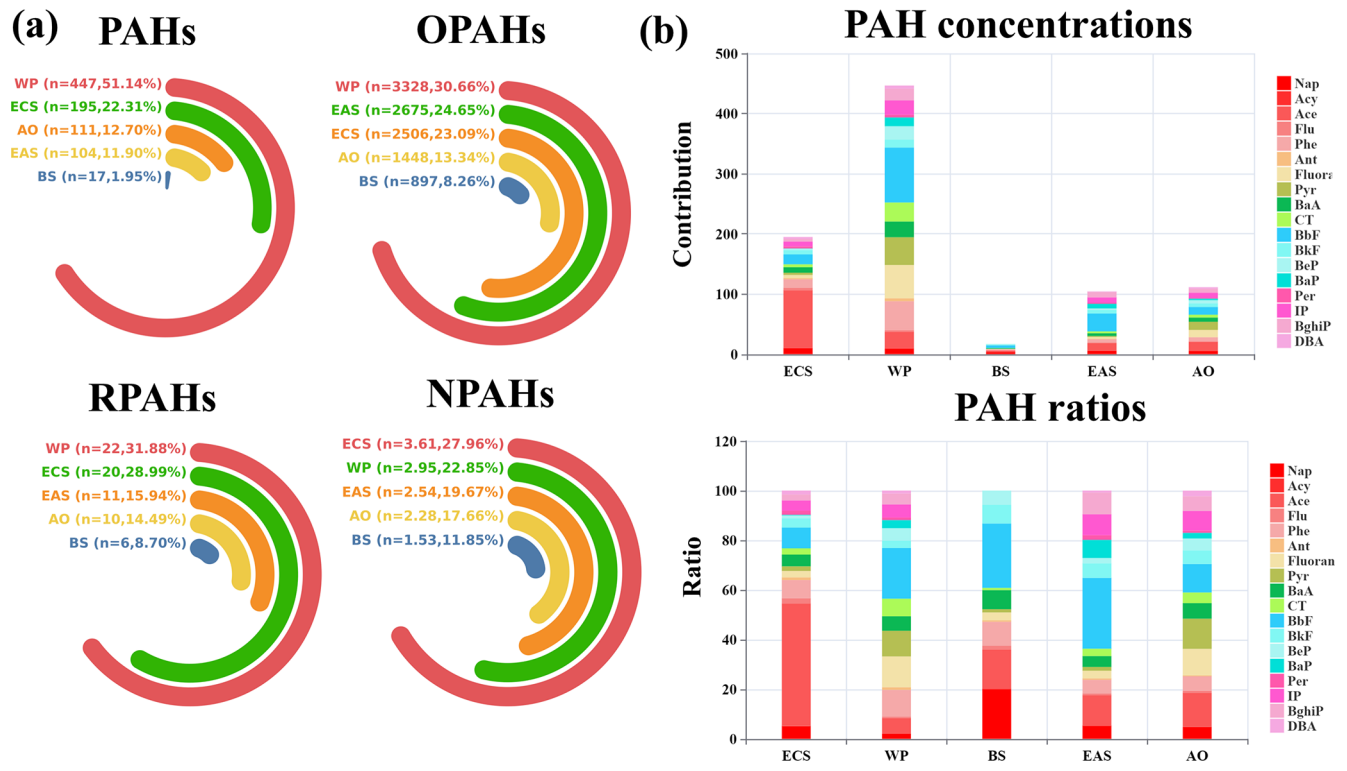

Figure 3. The spatial variations of PAHs and derivatives in the marine aerosols, where n represents the average concentration of PAHs and derivatives, and the ratio (%) denotes the quotient of PAH concentrations in each region and the total concentrations in all five regions **(a)**. The spatial distributions of PAH species (unit: pg m^{-3}) in the global marine aerosols are shown **(b)**.

summer and autumn of Australia (Haque et al., 2021), which might elevate the BbF concentration in the marine aerosol along Australia. The simulated wildfire-related ambient benzene concentration via the GEOS-Chem model (Fig. S2) was utilized to establish the relationship with the ambient BbF level in the aerosols, and the correlation coefficient reached 0.52 ($p < 0.05$). The result confirmed that local wildfire in Australia largely increased BbF concentrations in the marine aerosol.

The total OPAHs also exhibited marked spatial variations with the highest concentrations in the WP (3328 ± 1846 pg m^{-3}), followed by EAS (2675 ± 1452 pg m^{-3}), ECS (2506 pg m^{-3}), AO (1447±865 pg m^{-3}), and (the lowest one) BS (897±544 pg m^{-3}). Unlike the spatial distribution of parent PAHs, OPAH levels in the EAS were much higher than those in the AO and BS. It is widely acknowledged that OPAHs were mainly derived from the secondary formation of parent PAH and O_3 and OH radicals (Ambade et al., 2023). It was assumed that both O_3 and OH radicals were higher in the tropical oceans compared with the temperate and southern oceans based on the GEOS-Chem model (Fig. S3). The correlation analysis also suggested that the OPAH concentrations displayed a good relationship with the O_3 level ($r = 0.55$, $p < 0.05$). In addition, the ratios of OPAH/PAH in the ECS, WP, BS, EAS, and AO were 13, 7, 53, 26, and 13, respectively. We could find that the oxidation capacities of PAH in the BS and EAS were much higher compared with other oceans, though the primary emission of PAH in the BS was relatively low. All of these results demonstrated that the strong oxidation capacity of O_3 and OH radicals promoted the higher OPAH concentrations. Most of the OPAH species displayed similar spatial variations with the total OPAH concentrations, while few components such as 1-Naphthaldehyd, Ancenaphthenaquinone, and 6H-Benzo(cd)pyrene-6-one levels in the ECS were still higher than those in the EAS. This might be linked with the emission intensity of their precursors.

Both RPAHs and NPAHs showed higher levels in the ECS (20 and 3.6 pg m^{-3}) and WP (22 ± 13 and 3.0 ± 1.2 pg m^{-3}), which were significantly higher than those in other seas. Among all of the species of RPAHs and NPAHs, 1-Methylnaphthalene and 2-Nitronaphthalene exhibited significantly higher concentrations in the ECS (1.61 and 3.61 pg m^{-3}) and WP (2.1 ± 1.3 and 2.8 ± 1.1 pg m^{-3}) compared with other regions (Figs. S4 and S5) ($p < 0.05$). It has been well documented that both of these species were derived from diesel vehicle emissions. Southeast Asia and East Asia showed the higher diesel vehicle emissions of parent PAHs compared with Australia and some countries in the Southern Hemisphere (Shen et al., 2013).

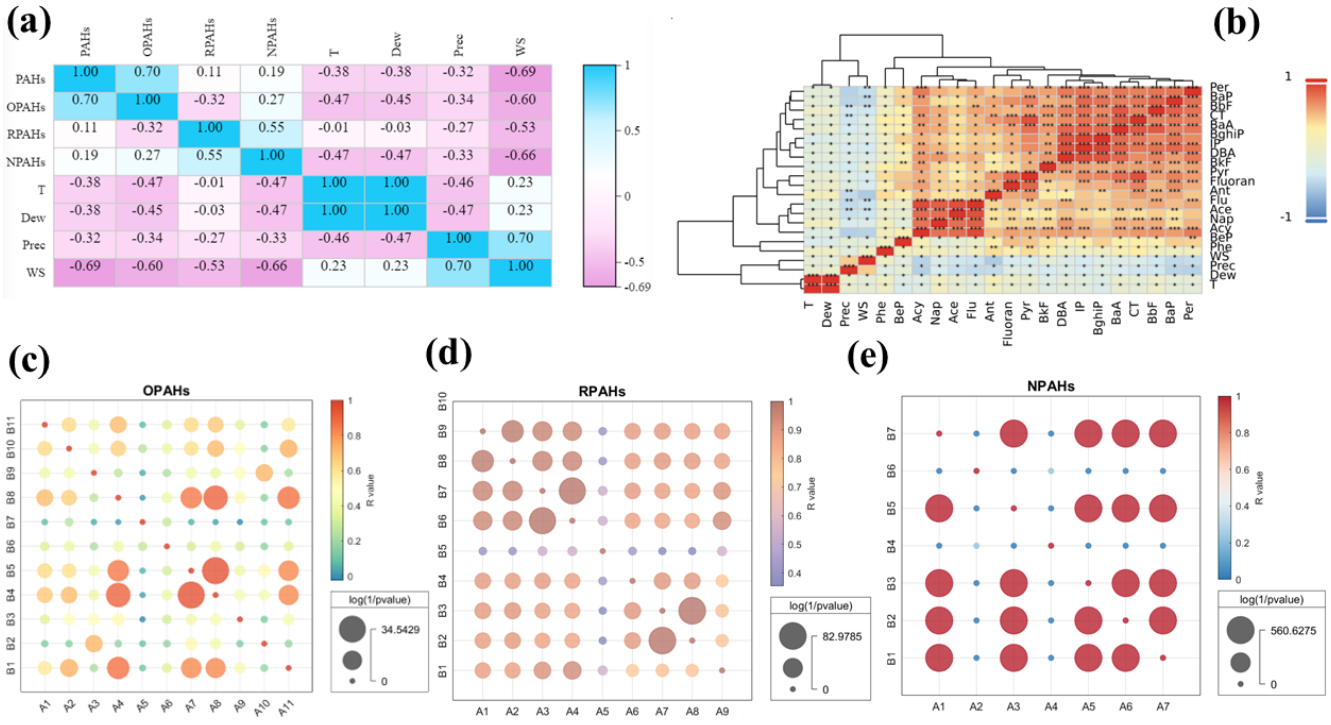

Figure 4. The correlation of PAHs, OPAHs, RPAHs, and NPAHs as well as meteorological parameters. The correlation of PAH species and meteorological factors **(b)**. The correlation coefficients and $\log(1/p)$ values of OPAH species **(c)**. A1 (B1), A2 (B2), A3 (B3), A4 (B4), A5 (B5), A6 (B6), A7 (B7), A8 (B8), A9 (B9), A10 (B10), and A11 (B11) in **(c)** represent 1,4-Naphthoquinone, 1-Naphthaldehyd, 1-Ancenaphthenaquinone, 9-Fluorenone, Ancenaphthenaquinone, Anthraquinone, Benzanthrone, Benzo(a) anthracene-7,12-dione, 1,4-Chysenequione, 5,12-Naphthacenequione, and 6H-Benzo(cd)pyrene-6-one, respectively. The correlation coefficients and $\log(1/p)$ values of RPAH species **(d)**. A1 (B1), A2 (B2), A3 (B3), A4 (B4), A5 (B5), A6 (B6), A7 (B7), A8 (B8), and A9 (B9) in **(d)** denote 2-Methylnaphthalene, 1-Methylnaphthalene, 2,6-Dimethylnaphthalene, 1,3-Dimethylnaphthalene, 1,6,7-Trimethylnaphthalene, 2-Methylanthracene, 1-Methylphenanthrene, 1-Methylanthracene, and 1-Methylfluoranthene, respectively. The correlation coefficients and $\log(1/p)$ values of NPAH species **(e)**. A1 (B1), A2 (B2), A3 (B3), A4 (B4), A5 (B5), A6 (B6), and A7 (B7) in **(e)** reflect 1-Nitronaphthalene, 2-Nitronaphthalene, 1,3-Dinitronaphthalene, 5-Nitroacenaphthene, 2-Nitrofluorene, 9-Nitroanthracene, and 1,8-Dinitronaphthalene, respectively.

Besides, some key meteorological factors including 2 m air temperature (T), 2 m dewpoint temperature (Dew), precipitation (Prec), and wind speed (WS) were also selected to assess their impacts on PAH derivatives (Fig. 4). The result suggested that most PAH derivatives showed significant negative correlation with nearly all of the meteorological parameters. Among all of the meteorological parameters, WS showed the highest correlation coefficients with all of the PAH derivatives, indicating that dilution and diffusion conditions significantly affected their fate, because most of these compounds showed relatively long lifetime. Besides, T also showed the higher negative correlation with PAH derivatives, because the gas–particle partitioning of PAHs was mainly controlled by the air temperature (Li et al., 2020; Wang et al., 2019b). High air temperature usually suppresses gaseous to particulate sorption of PAH derivatives to marine aerosol and compound-dependent adsorption kinetics in the atmosphere (Andreae, 1983; Gustafson and Dickhut, 1996; Wang et al., 2019a). Although rainfall washout might be an important pathway for PAH decrease, the correlation coefficients of Prec and PAH derivatives were slightly lower than other meteorological factors. It was assumed that the sampling period showed less rainfall events; thus, the PAH derivatives were not sensitive to Prec.

3.3 Source apportionment of parent PAH and derivatives

The diagnostic ratio between PAHs has been widely utilized to identify the major sources of particulate PAHs. Based on previous studies, the Fluoran/(Fluoran + Pyr) ratio could be applied to distinguish the potential sources. The ratios less than 0.4, 0.4–0.5, and greater than 0.5 could be treated as petrogenic source (< 0.4), petroleum combustion or biomass burning (0.4–0.5), and coal combustion (> 0.5), respectively (Yunker et al., 2002; Zhang et al., 2021a). In our study, the Fluoran/(Fluoran + Pyr) ratios in nearly all of the regions except AO (0.46) were higher than 0.5, indicating the impact of coal combustion on marine aerosols in most regions

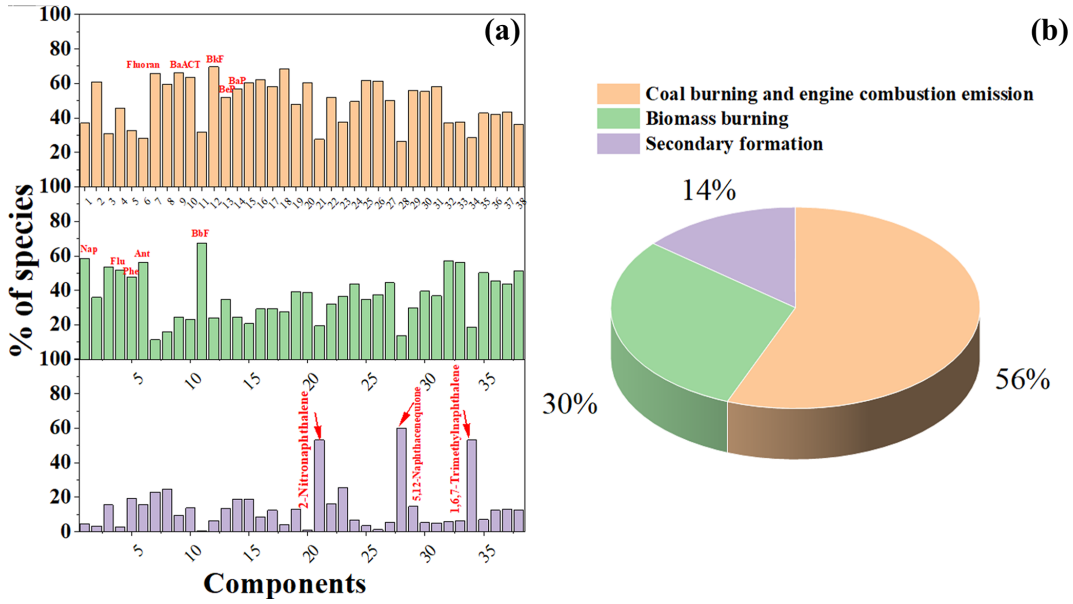

Figure 5. The factor profiles (% of species) resolved from PMF analysis **(a)**. Source contributions of three factors to the total parent PAHs and derivatives in $PM_{2.5}$ at the marine atmosphere **(b)**. The numbers from 1–38 denote Nap, Acy, Ace, Flu, Phe, Ant, Fluoran, Pyr, BaA, CT, BbF, BkF, BeP, BaP, Per, IP, BghiP, DBA, 1,4-Naphthoquinone, 1-Naphthaldehyd, 2-Nitronaphthalene, 1-Ancenaphthenaquinone, 9-Fluorenone, Ancenaphthenaquinone, Anthraquinone, Benzanthrone, Benzo(a) anthracene-7,12-dione, 1,4-Chysenequione, 5,12-Naphthacenequione, 6H-Benzo(cd)pyrene-6-one, 2-Methylnaphthalene, 1-Methylnaphthalene, 2,6-Dimethylnaphthalene, 1,3-Dimethylnaphthalene, 1,6,7-Trimethylnaphthalene, 2-Methylanthracene, 1-Methylphenanthrene, and 1-Methylanthracene, respectively.

in the Northern Hemisphere and tropical regions. The geochemical index method shows some uncertainties; thus, it is necessary to employ more diagnostic ratios to enhance the reliability. The BaP/BghiP ratio was also widely applied to separate the sources of vehicle emissions (≤ 0.6) and coal burning (> 0.6). Both BS (0.90) and EAS (0.84) showed higher BaP/BghiP ratios, indicating the important impact of coal combustion on the local marine aerosol (Katsoyiannis et al., 2007). However, the ratio in the ECS was much lower than 0.6, indicating that the vehicle or shipping emissions also play a significant role on the local aerosol. Meanwhile, the BaP/(BaP + CT) ratios in the ECS and WP reached 0.09 and 0.31, respectively. The result fills in the domain derived from diesel emissions, which further supports the inference that marine aerosols in both ECS and WP were significantly affected by diesel emissions (Ma et al., 2020). For the AO, all of the diagnostic ratios suggested that the oceans were mainly affected by shipping emission and wood burning.

Although the geochemical index method could identify the potential sources of PAH species, the contributions of multiple sources to PAHs and their derivatives still remained unknown. Therefore, positive matrix factorization (version PMF 5.0) was utilized to determine more source information of PAH species. After 30 runs, the optimal three factors with the lowest values of Q (robust) and Q (true) were determined. Factor 1 (56 %) possesses higher loadings of Fluoran, BaA, CT, BeP, BaP, and 1-Methylnaphthalene (Fig. 5). It is well known that Fluoran and BaA are typical indicators for coal combustion (Wang et al., 2016). Meanwhile, BeP, BaP, and 1-Methylnaphthalene are often derived from shipping emissions (Li et al., 2022). Therefore, factor 1 could be defined as the mixed source of coal burning and engine combustion emissions. Factor 2 (30 %) shows a high correlation with low-molecular-weight (LMW) PAHs such as Nap, Flu, Phe, Ant, and BbF. It is well documented that these LMW PAH species mainly originate from wood and biomass burning (Chen et al., 2022; Zhang et al., 2021a, 2020). Factor 3 (14 %) is characterized by medium and high contributions of 5,12-Naphthacenequione, 1,6,7-Trimethylnaphthalene, and 2-Nitronaphthalene. Many previous studies have confirmed that the photochemical reaction involving NO_2 initiated by OH radicals was highly effective for the production of 2-Nitronaphthalene in $PM_{2.5}$ (Arey et al., 1990; Atkinson et al., 1990). Hence, the factor could be treated to be the secondary formation. Based on the source apportionment, we verified that EAS showed a relatively high secondary contribution compared with some regions such ECS and WP. It was assumed that EAS showed the higher atmospheric oxidants and low PAH emissions (Ambade et al., 2023; Shen et al., 2013), which was in good agreement with the spatial variations of PAHs and OPAHs.

4 Conclusions and implications

In summary, our study verifies the ubiquitous occurrence of PAHs and their derivatives in the aerosols of the Western Pacific (WP), Bismarck Sea (BS), East Australian Sea (EAS), and even the Antarctic Ocean (AO). The highest PAH concentrations in marine aerosols were observed in the WP ($447 \pm 228\,pg\,m^{-3}$), followed by the East China Sea (ECS) ($195\,pg\,m^{-3}$), AO ($111 \pm 91\,pg\,m^{-3}$), EAS ($104 \pm 88\,pg\,m^{-3}$), and (the lowest) BS ($17 \pm 12\,pg\,m^{-3}$). PAH derivatives (e.g., OPAHs, RPAHs, and NPAHs) also showed higher concentrations in the WP. The spatial characteristics of these components can be related to precursor emissions and oxidation patterns (e.g., OH/NO_3 radicals, O_3).

For instance, the higher PAH and derivative concentrations observed in the WP were primarily due to higher anthropogenic emissions from coal and engine combustion. PAH concentrations in the AO were even higher than those in the EAS and BS, while OPAH levels in the EAS were much higher than those in the AO. It is widely acknowledged that OPAHs mainly originate from the secondary formation of parent PAHs through reactions with O_3 and OH radicals. The concentrations of O_3 and OH radicals are higher in tropical oceans compared to temperate and southern oceans.

Both geochemical index methods and the PMF model suggested that PAHs and their derivatives in global marine aerosols are controlled by three major sources: coal burning and engine combustion emissions (56 %), wood and biomass burning (30 %), and secondary formation (14 %). Marine aerosols in the ECS and WP were dominated by coal burning and engine combustion, while BS and EAS were mainly influenced by wildfires and coal combustion. AO was significantly affected by biomass burning and local shipping emissions.

However, this study has some limitations. Firstly, it focuses only on particle-phase PAHs and derivatives, while gas-phase PAH species were not measured. Additionally, data on PAHs in seawater were lacking. Future research should investigate gas–particle partitioning and the exchange processes between air and seawater phases in the global marine environment. Moreover, our study did not include cruise observations of marine aerosols in the Atlantic or Arctic oceans. Future studies should collect marine aerosols from all major oceans. Furthermore, measuring the concentrations of PAHs and derivatives in marine aerosols over multiple years will help analyze the impact of changes in anthropogenic emissions on these components, providing insight into their spatial distribution and fate (formation or removal mechanisms).

Data availability. The data presented in this study are available at the Zenodo data archive https://zenodo.org/records/14291911 (Li et al., 2025).

Supplement. The supplement related to this article is available online at https://doi.org/10.5194/acp-25-9263-2025-supplement.

Author contributions. Conceptualization: RL, XL, and GS; data curation: YubS, YumS, and YG; formal analysis: ZY, XL.

Competing interests. The contact author has declared that none of the authors has any competing interests.

Disclaimer. Publisher's note: Copernicus Publications remains neutral with regard to jurisdictional claims made in the text, published maps, institutional affiliations, or any other geographical representation in this paper. While Copernicus Publications makes every effort to include appropriate place names, the final responsibility lies with the authors.

Acknowledgements. This work was supported by the National Natural Science Foundation of China (42107113, 42276243) and the Fundamental Research Funds for the Central Universities. The authors are grateful to the CHINARE members for their support and assistance in atmosphere sampling.

Financial support. This research has been supported by the National Natural Science Foundation of China (grant no. 42107113).

Review statement. This paper was edited by Markus Ammann and reviewed by two anonymous referees.

References

Ambade, B., Sethi, S. S., and Chintalacheruvu, M. R.: Distribution, risk assessment, and source apportionment of polycyclic aromatic hydrocarbons (PAHs) using positive matrix factorization (PMF) in urban soils of East India, Environm Geochem. Hlth., 45, 491–505, 2023.

Andreae, M. O.: Soot carbon and excess fine potassium: Long-range transport of combustion-derived aerosols, Science, 220, 1148–1151, 1983.

Arey, J., Atkinson, R., Aschmann, S. M., and Schuetzle, D.: Experimental investigation of the atmospheric chemistry of 2-methyl-1-nitronaphthalene and a comparison of predicted nitroarene concentrations with ambient air data, Polycycl. Aromat. Comp., 1, 33–50, 1990.

Atkinson, R., Arey, J., Zielinska, B., and Aschmann, S. M.: Kinetics and nitro-products of the gas-phase OH and N_3 radical-initiated reactions of naphthalene-d8, Fluoranthene-d10, and pyrene, Int. J. Chem. Kinet., 22, 999–1014, 1990.

Bandowe, B. A. M. and Meusel, H.: Nitrated polycyclic aromatic hydrocarbons (nitro-PAHs) in the environment – a review, Sci. Total Environ., 581, 237–257, 2017.

Cabrerizo, A., Galbán-Malagón, C., Del Vento, S., and Dachs, J.: Sources and fate of polycyclic aromatic hydrocarbons in the Antarctica and Southern Ocean atmosphere, Global Biogeochem. Cy., 28, 1424–1436, 2014.

Chen, Y., Hall, J., van Wees, D., Andela, N., Hantson, S., Giglio, L., van der Werf, G. R., Morton, D. C., and Randerson, J. T.: Multi-decadal trends and variability in burned area from the fifth version of the Global Fire Emissions Database (GFED5), Earth Syst. Sci. Data, 15, 5227–5259, https://doi.org/10.5194/essd-15-5227-2023, 2023.

Chen, Y.-P., Zeng, Y., Guan, Y.-F., Huang, Y.-Q., Liu, Z., Xiang, K., Sun, Y.-X., and Chen, S.-J.: Particle size-resolved emission characteristics of complex polycyclic aromatic hydrocarbon (PAH) mixtures from various combustion sources, Environ. Res., 214, 113840, https://doi.org/10.1016/j.envres.2022.113840, 2022.

Gao, B., Wang, X.-M., Zhao, X.-Y., Ding, X., Fu, X.-X., Zhang, Y.-L., He, Q.-F., Zhang, Z., Liu, T.-Y., and Huang, Z.-Z.: Source apportionment of atmospheric PAHs and their toxicity using PMF: Impact of gas/particle partitioning, Atmos. Environ., 103, 114–120, 2015.

Gustafson, K. E. and Dickhut, R. M.: Particle/gas concentrations and distributions of PAHs in the atmosphere of southern Chesapeake Bay, Environ. Sci. Technol., 31, 140–147, 1996.

Hamal, K., Sharma, S., Khadka, N., Baniya, B., Ali, M., Shrestha, M. S., Xu, T., Shrestha, D., and Dawadi, B.: Evaluation of MERRA-2 precipitation products using gauge observation in Nepal, Hydrology, 7, 40, https://doi.org/10.3390/hydrology7030040, 2020.

Haque, M. K., Azad, M. A. K., Hossain, M. Y., Ahmed, T., Uddin, M., and Hossain, M. M.: Wildfire in Australia during 2019–2020, Its impact on health, biodiversity and environment with some proposals for risk management: a review, Journal of Environmental Protection, 12, 391–414, 2021.

Hoesly, R. M., Smith, S. J., Feng, L., Klimont, Z., Janssens-Maenhout, G., Pitkanen, T., Seibert, J. J., Vu, L., Andres, R. J., Bolt, R. M., Bond, T. C., Dawidowski, L., Kholod, N., Kurokawa, J.-I., Li, M., Liu, L., Lu, Z., Moura, M. C. P., O'Rourke, P. R., and Zhang, Q.: Historical (1750–2014) anthropogenic emissions of reactive gases and aerosols from the Community Emissions Data System (CEDS), Geosci. Model Dev., 11, 369–408, https://doi.org/10.5194/gmd-11-369-2018, 2018.

Iakovides, M., Iakovides, G., Stephanou, E. G.: Atmospheric particle-bound polycyclic aromatic hydrocarbons, *n*-alkanes, hopanes, steranes and trace metals: $PM_{2.5}$ source identification, individual and cumulative multi-pathway lifetime cancer risk assessment in the urban environment, Sci. Total Environ., 752, 141834, https://doi.org/10.1016/j.scitotenv.2020.141834, 2021.

Jaeckels, J. M., Bae, M.-S., and Schauer, J. J.: Positive matrix factorization (PMF) analysis of molecular marker measurements to quantify the sources of organic aerosols, Environ. Sci. Technol., 41, 5763–5769, 2007.

Kang, M., Yang, F., Ren, H., Zhao, W., Zhao, Y., Li, L., Yan, Y., Zhang, Y., Lai, S., and Zhang, Y.: Influence of continental organic aerosols to the marine atmosphere over the East China Sea: Insights from lipids, PAHs and phthalates, Sci. Total Environ., 607, 339–350, 2017.

Katsoyiannis, A., Terzi, E., and Cai, Q.-Y.: On the use of PAH molecular diagnostic ratios in sewage sludge for the understanding of the PAH sources. Is this use appropriate?, Chemosphere, 69, 1337–1339, 2007.

Koster, R. D., Reichle, R. H., Mahanama, S. P., Perket, J., Liu, Q., and Partyka, G.: Land-focused changes in the updated GEOS FP system (Version 5.25), 2020.

Kovacic, P. and Somanathan, R.: Nitroaromatic compounds: Environmental toxicity, carcinogenicity, mutagenicity, therapy and mechanism, J. Appl. Toxicol., 34, 810–824, 2014.

Li, B., Zhou, S., Wang, T., Zhou, Y., Ge, L., and Liao, H.: Spatio-temporal distribution and influencing factors of atmospheric polycyclic aromatic hydrocarbons in the Yangtze River Delta, J. Clean. Prod., 267, 122049, https://doi.org/10.1016/j.jclepro.2020.122049, 2020.

Li, C., Li, Z., and Wang, H.: Characterization and risk assessment of polycyclic aromatic hydrocarbons (PAHs) pollution in particulate matter in rural residential environments in China-A review, Sustain. Cities Soc., 104690, https://doi.org/10.1016/j.scs.2023.104690, 2023.

Li, D., Zhao, Y., Du, W., Zhang, Y., Chen, Y., Lei, Y., Wu, C., and Wang, G.: Characterization of $PM_{2.5}$-bound parent and oxygenated PAHs in three cities under the implementation of Clean Air Action in Northern China, Atmos. Res., 267, 105932, https://doi.org/10.1016/j.atmosres.2021.105932, 2022.

Li, R., Hua, P., and Krebs, P.: Global trends and drivers in consumption-and income-based emissions of polycyclic aromatic hydrocarbons, Environ. Sci. Technol., 56, 131–144, 2021a.

Li, R., Shen, Y., Shao, Y., Gao, Y., Yao, Z., Liu, Q., Liu, X., and Shi, G.: Measurement Report: Polycyclic aromatic hydrocarbons (PAHs) and their alkylated (RPAHs), nitrated (NPAHs) and oxygenated (OPAHs) derivatives in the global marine atmosphere: occurrence, spatial variations, and source apportionment, EGUsphere [preprint], https://doi.org/10.5194/egusphere-2024-3740, 2025.

Li, Y., Liu, M., Hou, L., Li, X., Yin, G., Sun, P., Yang, J., Wei, X., He, Y., and Zheng, D.: Geographical distribution of polycyclic aromatic hydrocarbons in estuarine sediments over China: Human impacts and source apportionment, Sci. Total Environ., 768, 145279, 2021b.

Li, R., Liu, X., Shen, Y. B., Shao, Y. M., Gao, Y. N., Yao, Z. W., Liu, X., and Shi, G.: Measurement report: Polycyclic aromatic hydrocarbons (PAHs) and their alkylated (RPAHs), nitrated (NPAHs), and oxygenated (OPAHs) derivatives in the global marine atmosphere – occurrence, spatial variations, and source apportionment, Zenodo [data set], https://zenodo.org/records/14291911 (last access: 25 May 2025), 2025.

Ma, L., Li, B., Liu, Y., Sun, X., Fu, D., Sun, S., Thapa, S., Geng, J., Qi, H., and Zhang, A.: Characterization, sources and risk assessment of $PM_{2.5}$-bound polycyclic aromatic hydrocarbons (PAHs) and nitrated PAHs (NPAHs) in Harbin, a cold city in Northern China, J. Clean. Prod., 264, 121673, https://doi.org/10.1016/j.jclepro.2020.121673, 2020.

Murray, L. T., Jacob, D. J., Logan, J. A., Hudman, R. C., and Koshak, W. J.: Optimized regional and interannual variability of lightning in a global chemical transport model constrained by LIS/OTD satellite data, J. Geophys. Res.-Atmos., 117, D20307, https://doi.org/10.1029/2012JD017934, 2012.

Neroda, A. S., Goncharova, A. A., and Mishukov, V. F.: PAHs in the atmospheric aerosols and seawater in the North–West Pa-

cific Ocean and Sea of Japan, Atmos. Environ., 222, 117117, https://doi.org/10.1016/j.atmosenv.2019.117117, 2020.

Park, R. J., Jacob, D. J., Field, B. D., Yantosca, R. M., and Chin, M.: Natural and transboundary pollution influences on sulfate-nitrate-ammonium aerosols in the United States: Implications for policy, J. Geophys. Res.-Atmos., 109, D15204, https://doi.org/10.1029/2003JD004473, 2004.

Pietrogrande, M. C., Abbaszade, G., Schnelle-Kreis, J., Bacco, D., Mercuriali, M., and Zimmermann, R.: Seasonal variation and source estimation of organic compounds in urban aerosol of Augsburg, Germany, Environ. Pollut., 159, 1861–1868, 2011.

Qiu, Y., Ma, Z., Li, K., Lin, W., Tang, Y., Dong, F., and Liao, H.: Markedly enhanced levels of peroxyacetyl nitrate (PAN) during COVID-19 in Beijing., Geophys. Res. Lett., 47, e2020GL089623, https://doi.org/10.1029/2020GL089623, 2020.

Sevimoglu, O. and Rogge, W. F.: Seasonal size-segregated PM_{10} and PAH concentrations in a rural area of sugarcane agriculture versus a coastal urban area in Southeastern Florida, USA, Particuology, 28, 52–59, 2016.

Sharma, S., Mandal, T., Jain, S., Saraswati, Sharma, A., and Saxena, M.: Source apportionment of $PM_{2.5}$ in Delhi, India using PMF model, B. Environ. Contam. Tox. 97, 286–293, 2016.

Shen, H., Huang, Y., Wang, R., Zhu, D., Li, W., Shen, G., Wang, B., Zhang, Y., Chen, Y., and Lu, Y.: Global atmospheric emissions of polycyclic aromatic hydrocarbons from 1960 to 2008 and future predictions, Environ. Sci. Technol. 47, 6415–6424, 2013.

Taghvaee, S., Sowlat, M. H., Mousavi, A., Hassanvand, M. S., Yunesian, M., Naddafi, K., and Sioutas, C.: Source apportionment of ambient $PM_{2.5}$ in two locations in central Tehran using the Positive Matrix Factorization (PMF) model, Sci. Total Environ., 628, 672–686, 2018.

Van Overmeiren, P., Demeestere, K., De Wispelaere, P., Gili, S., Mangold, A., and De Causmaecker, K., Mattielli, N., Delcloo, A., Langenhove, H. V., Walgraeve, C.: Four Years of Active Sampling and Measurement of Atmospheric Polycyclic Aromatic Hydrocarbons and Oxygenated Polycyclic Aromatic Hydrocarbons in Dronning Maud Land, East Antarctica, Environ. Sci. Technol., 58, 1577–1588, 2024.

Wang, J., Ho, S. S. H., Huang, R., Gao, M., Liu, S., Zhao, S., Cao, J., Wang, G., Shen, Z., and Han, Y.: Characterization of parent and oxygenated-polycyclic aromatic hydrocarbons (PAHs) in Xi'an, China during heating period: An investigation of spatial distribution and transformation, Chemosphere, 159, 367–377, 2016.

Wang, L., Dong, S., Liu, M., Tao, W., Xiao, B., Zhang, S., Zhang, P., and Li, X.: Polycyclic aromatic hydrocarbons in atmospheric $PM_{2.5}$ and PM_{10} in the semi-arid city of Xi'an, Northwest China: Seasonal variations, sources, health risks, and relationships with meteorological factors, Atmos. Res., 229, 60–73, 2019a.

Wang, Y., Zhang, Q., Zhang, Y., Zhao, H., Tan, F., Wu, X., and Chen, J.: Source apportionment of polycyclic aromatic hydrocarbons (PAHs) in the air of Dalian, China: Correlations with six criteria air pollutants and meteorological conditions, Chemosphere, 216, 516–523, 2019b.

Weagle, C. L., Snider, G., Li, C., van Donkelaar, A., Philip, S., Bissonnette, P., Burke, J., Jackson, J., Latimer, R., and Stone, E.: Global sources of fine particulate matter: interpretation of $PM_{2.5}$ chemical composition observed by SPARTAN using a global chemical transport model, Environ. Sci. Technol., 52, 11670–11681, 2018.

Wei, C., Bandowe, B. A. M., Han, Y., Cao, J., Watson, J. G., Chow, J. C., and Wilcke, W.: Polycyclic aromatic compounds (PAHs, oxygenated PAHs, nitrated PAHs, and azaarenes) in air from four climate zones of China: Occurrence, gas/particle partitioning, and health risks, Sci. Total Environ., 786, 147234, https://doi.org/10.1016/j.scitotenv.2021.147234, 2021.

Wietzoreck, M., Kyprianou, M., Musa Bandowe, B. A., Celik, S., Crowley, J. N., Drewnick, F., Eger, P., Friedrich, N., Iakovides, M., Kukučka, P., Kuta, J., Nežiková, B., Pokorná, P., Přibylová, P., Prokeš, R., Rohloff, R., Tadic, I., Tauer, S., Wilson, J., Harder, H., Lelieveld, J., Pöschl, U., Stephanou, E. G., and Lammel, G.: Polycyclic aromatic hydrocarbons (PAHs) and their alkylated, nitrated and oxygenated derivatives in the atmosphere over the Mediterranean and Middle East seas, Atmos. Chem. Phys., 22, 8739–8766, https://doi.org/10.5194/acp-22-8739-2022, 2022.

Yan, Y., He, Q., Guo, L., Li, H., Zhang, H., Shao, M., and Wang, Y.: Source apportionment and toxicity of atmospheric polycyclic aromatic hydrocarbons by PMF: Quantifying the influence of coal usage in Taiyuan, China, Atmos. Res., 193, 50–59, 2017.

Yunker, M. B., Macdonald, R. W., Vingarzan, R., Mitchell, R. H., Goyette, D., and Sylvestre, S.: PAHs in the Fraser River basin: a critical appraisal of PAH ratios as indicators of PAH source and composition, Org. Geochem., 33, 489–515, 2002.

Zetterdahl, M., Moldanova, J., Pei, X. Y., Pathak, R. V., and Demirdjian, B.: Impact of the 0.1 % fuel sulfur content limit in SECA on particle and gaseous emissions from marine vessels, Atmos. Environ., 145, 338–345, 2016.

Zhang, L., Yang, L., Bi, J., Liu, Y., Toriba, A., Hayakawa, K., Nagao, S., and Tang, N.: Characteristics and unique sources of polycyclic aromatic hydrocarbons and nitro-polycyclic aromatic hydrocarbons in $PM_{2.5}$ at a highland background site in northwestern China⋆, Environ. Pollut., 274, 116527, https://doi.org/10.1016/j.envpol.2021.116527, 2021a.

Zhang, L., Yang, L., Zhou, Q., Zhang, X., Xing, W., Wei, Y., Hu, M., Zhao, L., Toriba, A., and Hayakawa, K.: Size distribution of particulate polycyclic aromatic hydrocarbons in fresh combustion smoke and ambient air: A review, J. Environ. Sci., 88, 370–384, 2020.

Zhang, P., Zhou, Y., Chen, Y., Yu, M., and Xia, Z.: Construction of an atmospheric PAH emission inventory and health risk assessment in Jiangsu, China, Air Qual. Atmos. Hlth., 16, 629–640, 2023.

Zhang, X., Zhang, Z.-F., Zhang, X., Zhu, F.-J., Li, Y.-F., Cai, M., and Kallenborn, R.: Polycyclic aromatic hydrocarbons in the marine atmosphere from the Western Pacific to the Southern Ocean: Spatial variability, Gas/particle partitioning, and source apportionment, Environ. Sci. Technol., 56, 6253–6261, 2022a.

Zhang, Y., Shen, Z., Sun, J., Zhang, L., Zhang, B., Zou, H., Zhang, T., Ho, S. S. H., Chang, X., and Xu, H.: Parent, alkylated, oxygenated and nitrated polycyclic aromatic hydrocarbons in $PM_{2.5}$ emitted from residential biomass burning and coal combustion: A novel database of 14 heating scenarios, Environ. Pollut., 268, 115881, https://doi.org/10.1016/j.envpol.2020.115881, 2021c.

Zhang, Y. and Tao, S.: Global atmospheric emission inventory of polycyclic aromatic hydrocarbons (PAHs) for 2004, Atmos. Environ., 43, 812–819, 2009.

Zimmermann, K., Jariyasopit, N., Massey Simonich, S. L., Tao, S., Atkinson, R., and Arey, J.: Formation of nitro-PAHs from the heterogeneous reaction of ambient particle-bound PAHs with $N_2O_5/N_3/N_2$, Environ. Sci. Technol., 47, 8434–8442, 2013.